Fabrication and Characterization of Polyvinyl Alcohol/ TiO_2 Membrane immersed in Simulated Body Fluid for Biomedical Application

Dien Thi My Nguyen [1, 2], Khanh Do Gia Huynh [1, 2], Thuy Thanh Doan Nguyen[1, 2], Vu Tan Huynh [1,2*], Phuong Tuyet Nguyen[1, 2*] and Linh Thuy Ba Nguyen[3, *].

[1] *Faculty of Chemistry, University of Science, Nguyen Van Cu Street, Ho Chi Minh City, Vietnam*

[2] *Vietnam National University Ho Chi Minh City, Vietnam*

[3] *Division of Biomaterials and Tissue Engineering, Eastman Dental Institute, University College London, Royal Free Hospital, London, United Kingdom.*

*Corresponding author:

Email: l.nguyen@ucl.ac.uk (Linh Thuy Ba Nguyen)

ntphuong@hcmus.edu.vn (Phuong Tuyet Nguyen)

htvu@hcmus.edu.vn (Vu Tan Huynh)

ABSTRACT

In this study, we synthesized of hydroxyapatite (HA) on polyvinyl alcohol (PVA)/TiO_2 in which TiO_2 was prepared by the sol-gel method. HA was formed by immersing the membrane in the simulated body fluid (SBF) solution. We improved the mechanical strength of the membranes by adding glutaraldehyde (GA) combining with heat treatment to cross-link the polymer network. In addition, the composition of TiO_2 crystalline phase, TiO_2 content in each membrane, and the duration of membrane immersion in SBF solution were investigated. The morphological structures of HA/PVA/TiO_2 membranes were characterized by IR, SEM, and XRD. We confirmed that the HA formation depended on the TiO_2 content and phase composition (rutile or anatase). Membranes containing TiO_2 rutile-phase showed more pronounced HA formation than membranes containing TiO_2 anatase-phase. The appearance of HA also depended on SBF immersion duration. Membranes soaked for 3 weeks showed significantly more HA formation than membranes soaked for 1 and 2 weeks. Furthermore, the number of cells in membranes soaked for 3 weeks was clearly higher than in other membranes. Finally, HA/PVA/TiO_2 membranes containing 25 wt. % of TiO_2 rutile-phase are biocompatible based on the number of viable cells and thus have the potential for biomedical application.

Keywords: PVA/TiO_2, membrane, simulated body fluid, SBF, biomedical application

1 INTRODUCTION

Hydroxyapatite (HA) has a chemical composition and porous structure similar to human bone. It is highly biocompatible with cells and directly bonds the immature bone, leading to rapid bone regeneration [1]. Scientists extensively study the synthesis of HA itself to optimize the material [2, 3]. To improve its biological activity, the researchers also combine HA with other biological materials, typically in combination with titanium compounds commonly used in dentistry [4].

TiO_2 is considered a potential material in combination with HA among titanium compounds. TiO_2 is known for its anatase, rutile and brookite phases, but anatase and rutile phases are the most widely used [5, 6]. In addition to its optical and electrochemical properties, TiO_2 also has other unique properties applied in biomedical fields, such as biocompatibility [7]. On the other hand, PVA is a hydrophilic polymer with many advantages such as chemical resistance, excellent biocompatibility, good biodegradability and high-water permeability [5]. PVA/TiO_2 membranes are effectively used to fabricate scaffolds with appropriate mechanical strength[10.1002/adv.22167]. Combining HA and PVA/TiO_2 through immersion in simulated body fluid (SBF) will overcome the disadvantage of material separation [5]. HA synthesis that imitates physiological processes in the human body is reported to be more biocompatible than HA prepared directly from calcium and phosphate, followed by high-temperature plasma injection onto the substrate [1, 3, 8].

There have been many experiments demonstrating the ability of HA/PVA/TiO_2 membranes to support cell growth. Previous studies often investigated only one TiO_2 phase composition (anatase or rutile), TiO_2 content, or membrane immersion time in SBF [5, 9]. So far, no research has clearly explained the reason for choosing one TiO_2 phase from another. Most of the research only performed partial characterization by observing one of these three factors, either TiO_2 phase composition (anatase or rutile), TiO_2 content or membrane immersion time in SBF [1, 5, 8-10]. We hypothesized that all three factors have different influences on the results of cell formation.

This paper aims to synthesize HA on PVA/TiO_2 membrane, thereby confirming the HA forming ability of TiO_2 and the biocompatibility of the generated material. The experimental plan consisted of

- Synthesis of rutile and anatase TiO_2 by sol-gel method,
- Fabrication of PVA/TiO_2 membranes for each phase with different ratios,
- Preparation of stable membranes in an aqueous medium by crosslinking method,
- Investigation of HA formation on PVA/TiO_2 membranes with different TiO_2 content immersed in SBF solution in different time scales, and
- Investigation of the effect of HA on membrane biocompatibility with in vitro human skin fibroblasts cell culture.

2 Experimental procedure

2.1 Materials

Titanium tetrachloride ($TiCl_4$, MACKLIN China, 99.995%), ethanol (C_2H_5OH, Xilong, China, 99.95%), acetic acid (CH_3COOH, Xilong, China, 99.5%), ammonium hydroxide (NH_4OH, Xilong, China), polyvinyl alcohol (PVA, $[CH_2CH(OH)]_n$, HIMEDIA India), glutaraldehyde ($OCH(CH_2)_3CHO$, MERCK Germany), acetone (CH_3COCH_3, SK

CHEMICAL, Korea), hydrochloric acid (HCl, Duc Giang, Vietnam, 35~38%), human dermal fibroblast (HDF) cells (C0135C) (ThermoFisher Scientific, UK), Dulbecco's Modified Eagle Medium (DMEM) (ThermoFisher Scientific, UK), foetal bovine serum (FBS, ThermoFisher Scientific, UK), penicillin (ThermoFisher Scientific, UK), streptomycin (PS, ThermoFisher Scientific, UK), phosphate buffer saline (PBS, ThermoFisher Scientific, UK), sodium chloride (NaCl, GHTECH China, 99.5%) , sodium hydrogen carbonate ($NaHCO_3$, GHTECH, 99.5%), potassium chloride (KCl, Xilong, China), di-potassium hydrogen phosphate trihydrate ($K_2HPO_4.3H_2O$, Xilong, China, 99.0%), magnesium chloride hexahydrate ($MgCl_2.6H_2O$, Guangdong Guanghua, China, 98.0%), calcium chloride dihydrate ($CaCl_2.2H_2O$, Guangdong Guanghua, China, 98.0%) and sodium sulfate anhydrous (Na_2SO_4, Xylong, China, 99.0%) were used.

2.2 TiO_2 synthesis

5.0 mL $TiCl_4$ 1M as the precursor was taken into a beaker containing 14.0 mL ethanol, and the mixture was stirred at 700 rpm stirring speed and heated to 90℃. CH_3COOH and NH_4OH were used to adjust the pH value of solutions to 1 and 8, respectively. The stirrer was then turned off. The solution was left for 24 h to begin the gel aging process. After 24 h, the precipitate was filtered and washed several times with distilled water and ethanol, then dried at 80℃ for 3 h and then calcined at 500℃ for 4 h. Both products prepared at two different pH were obtained as white powders. The resulting sample was labeled as TiO_2-pH1 and TiO_2-pH8 for the sample prepared at pH = 1 and pH = 8, respectively.

2.3 PVA/TiO_2 membrane synthesis

The PVA/TiO_2 membranes made from different phases of TiO_2 have been prepared using the doctor blade method with different contents of TiO_2, including 5 wt.%, 10 wt.%, 15 wt.%, 20 wt.% and 25 wt.%. 2 mL water was added to TiO_2, and the solution was stirred for 4 h. Simultaneously, 3 mL of water was added to 1 g PVA, and then the solution was stirred and heated 90℃ for 4 h. Two resulting solutions were mixed, and the mixture was sonicated and stirred for 4 h. Each PVA/TiO_2 composite membrane formed on a piece of glass was dried at 100℃ for 3 h. After that, the membranes were soaked in mixed glutaraldehyde (GA)/HCl/acetone solution (1:1) (GA content = 1.0 v/v%) at 40 ℃ for 3 h to prevent water solubility of the membranes by chemical crosslinking. These membranes were immersed overnight in distilled water to remove impurities and then stored in a 1 N HCl solution.

In this research, we abbreviated the name of PVA membranes crosslinked by GA as "GP", PVA/TiO_2 membranes not crosslinked by GA as "PT", and PVA/TiO_2 membranes crosslinked by GA as "GPT". In addition, the name of membrane type is sometimes followed by the abbreviation of the TiO_2 phase prepared, such as "R" for rutile and "A" for anatase, together with TiO_2 content.

2.4 Hydroxyapatite formation on PVA/TiO_2 membranes in SBF solution

The SBF solution has been known as a supersaturated solution that can lead to apatite precipitation. The reagents for SBF include NaCl, $NaHCO_3$, KCl, $K_2HPO_4.3H_2O$, $MgCl_2.6H_2O$, $CaCl_2$, Na_2SO_4, $(HOCH_2)_3CNH_2$ (Tris), HCl 1N. The ion concentrations of all chemicals were controlled to have the similar ones in human blood plasma [11]. After that, the membranes were soaked in SBF solution with different time points: 1 week, 2 weeks and 3 weeks. The amount of SBF solution added to each 1.5-mL Eppendorf tube was 1 mL. In the

first 10 days, the SBF solution was changed with new ones every day to ensure the correct concentration of ions needed to form HA crystals. After this period, the SBF solution was changed every 5 days to keep the stability of HA crystal growth.

2.5 Materials characterization

The crystallite structure of the TiO_2 powders was evaluated by a Bruker D8 ADVANCE diffractometer using Cu Kα radiation (λ = 1.5418 Å) at 40 kV and 40 mA by scanning at 0.02°/S. FTIR spectra of the TiO_2 and membrane samples were obtained in Bruker VERTEX 70V at wavenumber ranging from 500 to 4000 cm^{-1}. TiO_2 spectra were obtained in KBr pellets before FTIR measurement, and membranes were analyzed using ATR (attenuated total reflection) modes. Their morphology was studied by performing scanning electron microscopy (SEM) with a Zeiss EVO HD microscope. The SEM samples were cut into discs (n=2) and then coated with 95% gold and 5% palladium (Polaron E5000 Sputter Coater, Quorum Technologies, UK).

The interaction of water with the pure PVA and composite membranes was measured and compared using a Contact Angle Measuring System (KSV CAM200 Optical Contact Angle Meter, Biolin Scientific, UK) at room temperature (19℃). The membranes were placed on a sample stage, and a water droplet was dropped automatically onto the surface of the sample to observe the water contact angle. A thin needle was used to make sessile drops. The drop was illuminated from one side, and the image of the drop was recorded by a camera on the opposite side of the instrument. The drop image was transferred to a computer and shown on the monitor. The CAM software analyzed the drop image to calculate the contact angle.

2.6 Cell viability

Human Dermal Fibroblast (HDF) cells were cultured in flasks with DMEM supplemented with 10% fetal bovine serum and 100 U/mL of penicillin, and 100 μg/mL of streptomycin under standard cell culture conditions (37℃, 5% CO_2, 95% humidity).

LIVE/DEAD staining is a dye-based assay that can provide a direct viability assessment, whereby cells are either alive (green) or dead (red). HDF cells were seeded onto the control and rutile-phase GA/PVA and GA/PVA/TiO_2 membrane samples in 48-well plates with a cell density of 10.000 cells/mL/sample. First, 0.5 mL of media was added to each well. The media was discarded, and the samples were washed with PBS at each timepoint. Next, prepare the dye solution: stock solution of EthD-1 (20 μL, 2 mM) was added to PBS (10 mL), and this mixture was combined with calcein-AM stock solution (5 μL, 4 mM) to prepare the stain. Finally, 500 μL of this reagent was added to each well and incubated for 20 minutes at room temperature. Cell viability was observed and evaluated using fluorescence microscopy (LEICA Instruments, Milton Keynes, UK) on Image Capture Pro software.

3 Result and discussion

3.1 Synthesis of TiO_2

3.1.1 XRD results

Figure 1 shows the XRD patterns of TiO_2 powders prepared at pH = 1 (TiO_2-pH1) and pH = 8 (TiO_2-pH8). In detail, the XRD pattern of TiO_2-pH1 exhibited diffraction peaks at 27.4°, 36.1°, 41.2°, 54.3°, 56.6°, and 69.0° indicating TiO_2 in the rutile phase with the corresponding

(110), (101), (111), (211), (220), and (112) planes, respectively. The peaks of TiO_2-pH8 were observed at 25.4°, 37.9°, 48.1°, 54.1°, and 62.7°, indicating TiO_2 in the anatase phase with the corresponding (101), (004), (200), (105), and (204) planes, respectively.

The crystallite size of the particles has been estimated from the Debye–Scherrer's equation using the XRD line broadening as follows [12]:

$$d = \frac{k\lambda}{\beta\cos(\theta)}$$

Where d is the average size of the particle, k is a constant (0.89), λ is the X-ray wavelength, β is the full width at half-maximum (in radians), and θ is the maximum angle of diffraction. The (101) plane diffraction peak is used for anatase and the (110) one for rutile. The TiO_2-pH1 and TiO_2-pH8 crystallite sizes are 73 and 35 nm, respectively.

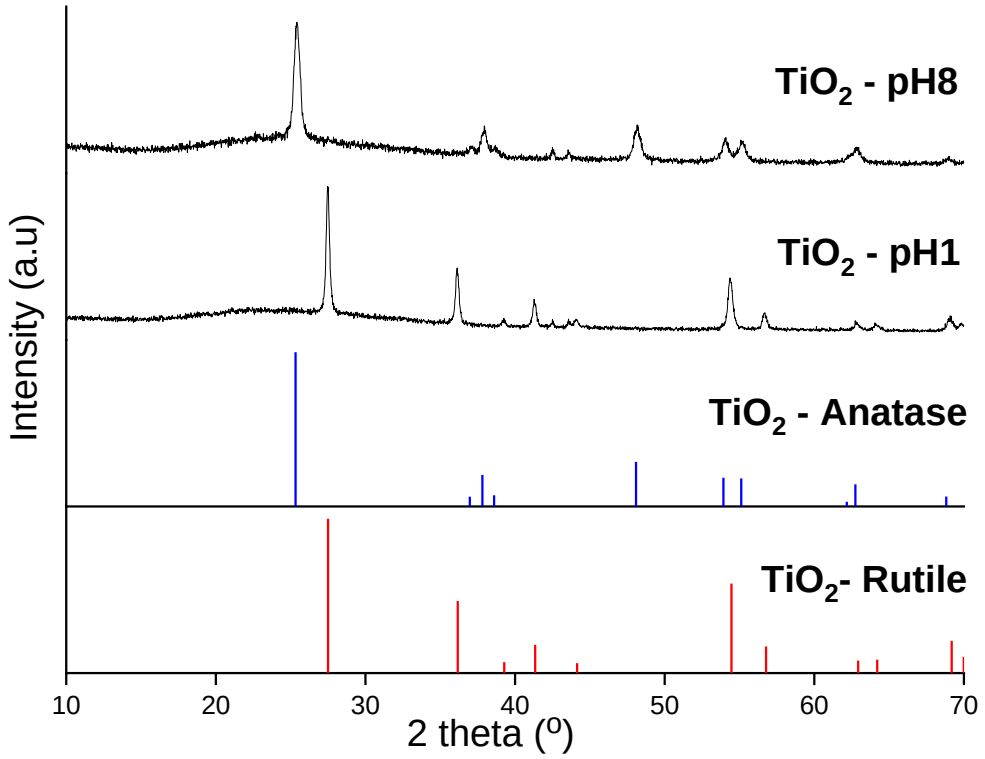

Figure 1. XRD patterns of TiO_2 powders prepared at: pH = 1 (TiO_2-pH1) and pH = 8 (TiO_2-pH8)

In previous experiments, the rutile phase of TiO_2 requires a 650 °C temperature to transform completely from the anatase to the rutile [13]. However, in this experiment, the calcined temperature in both experiments was at 500 °C. Therefore, we believe that the pH changes the structure arrangement to form TiO_2 crystals during nucleation and growth. Furthermore, Qinghong Zhang et al. suggested that the formation of rutile requires a relatively low rate and is controlled kinetically in the acid environment, so when adding NH_4OH solution to the mixture, the precipitation appeared immediately. This reaction made the equilibrium between the nucleation and the growth broken, suitable for forming anatase structure [13].

3.1.2 FTIR results

Figure 2 presents FTIR spectra of the TiO_2 powder samples of TiO_2-pH1 or TiO_2-pH8. The peak of the two samples reached a value of about 3000 - 3700 cm^{-1} due to the valence vibration of the -OH group on the surface, implying that $TiCl_4$ reacted with residual water in ethanol to form Ti-OH bond [14]. The bands between 500 – 700 cm^{-1} correspond to Ti-O and Ti-O-Ti stretching vibration.

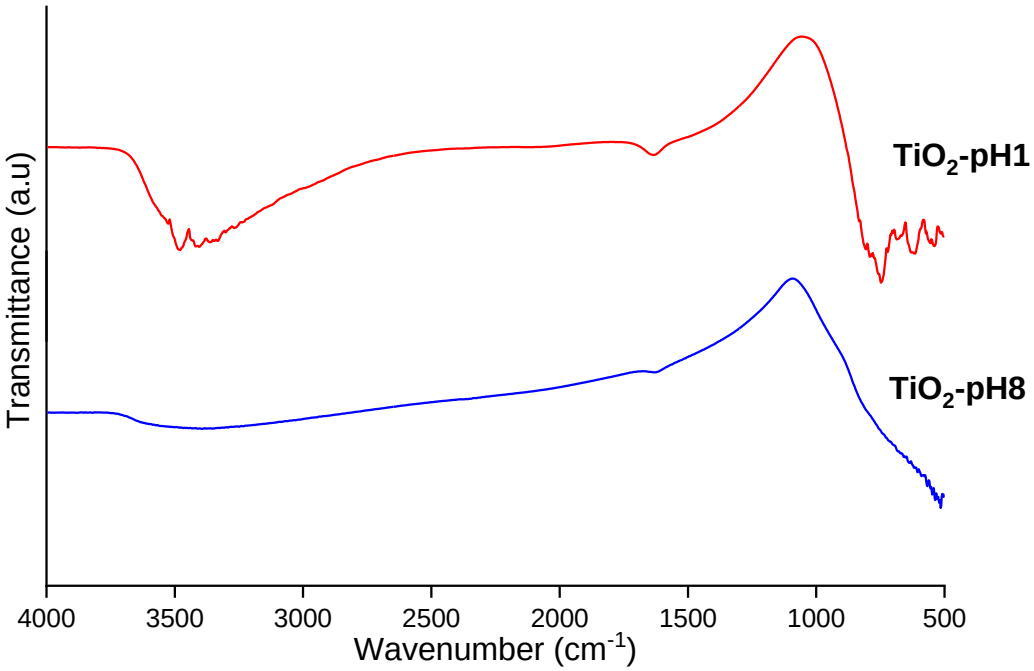

Figure 2. FTIR spectra of TiO_2 powders prepared at: pH = 1 (TiO_2-pH1) and pH = 8 (TiO_2-pH8)

3.1.3 SEM results

SEM analysis shows the particle size and morphology of TiO_2 samples, as indicated in **Figure 3.** TiO_2-pH1 shows that the rutile sample has a spherical shape, and its size typically ranges from 2 – 3 μm, while TiO_2-pH8 demonstrates most of the anatase particles are of unequal size. A very large agglomeration between the particles is found to form amorphous shape.

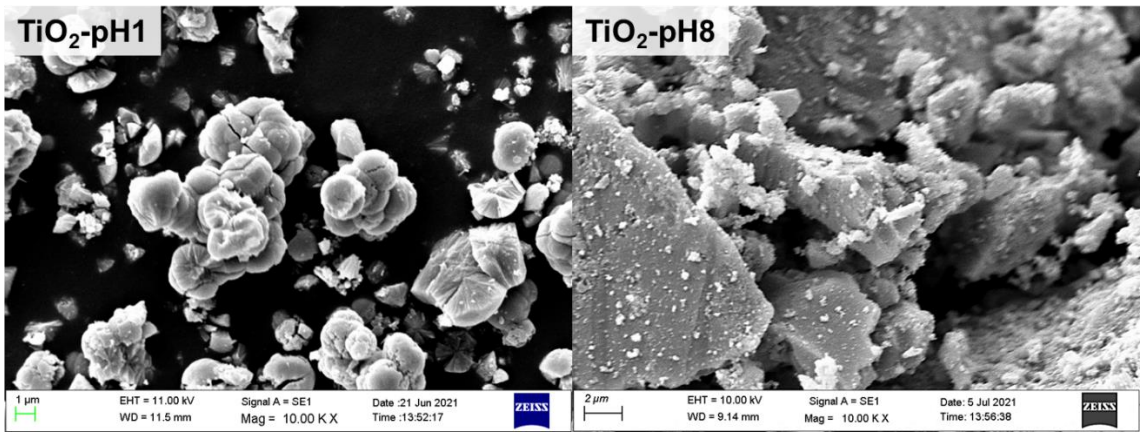

Figure 3. SEM images of TiO_2 prepared at: pH = 1 (TiO_2-pH1) and pH = 8 (TiO_2-pH1)

3.2 PVA membrane crosslinking mechanism

3.2.1 Crosslinking mechanism

Water permeates the PVA membrane mainly through ion channels, and thus the cross-sectional size of these channels determines the water permeability [15-17]. This size depends mainly on the swelling properties of the membrane. Thus, swelling facilitates the permeation of water and protons to some extent. The OH groups of PVA will form hydroxyl bonds with GA forming a hydrophobic barrier to provide the polymer with morphological stability and prevent the polymer from dissolving in solvents [16].

Observing the resulting PVA and PVA/TiO_2 membranes **(Figure 4, 5, 6)**, we can see that the similarity between the membranes is that after crosslinking with GA, the membrane length is shorter but swollen and yellowish than the uncross-linked membrane by GA. This can be explained by the fact that GA only binds with the polymer network of PVA in the outer layer and blocks hydroxyl groups on the surface. The shrinkage of the distance between the PVA chains due to the lattice structure causes the PVA and the TiO_2 molecules to accumulate, causing the membrane to stretch vertically.

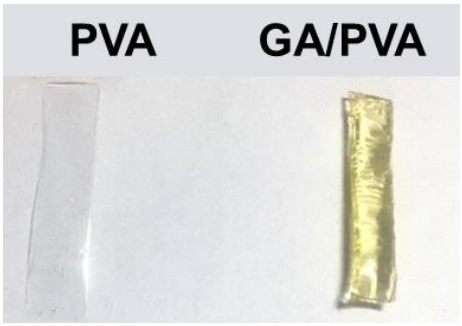

Figure 4. PVA membrane: Left - membrane without crosslinked; Right – membrane crosslinked with GA.

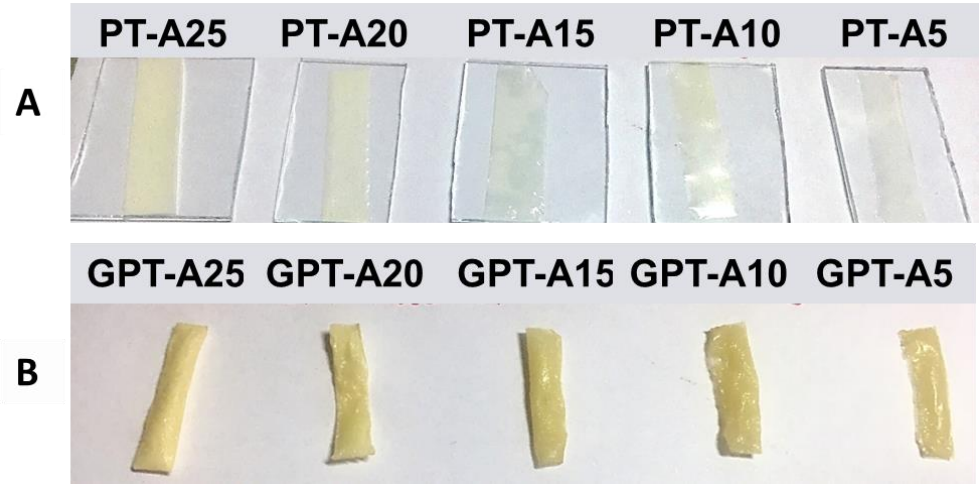

Figure 5. PVA/TiO_2 anatase membrane at TiO_2 contents, respectively (from left to right): 25%, 20%, 15%, 10% and 5%: A - membranes without crosslinked ; B – membranes crosslinked by GA.

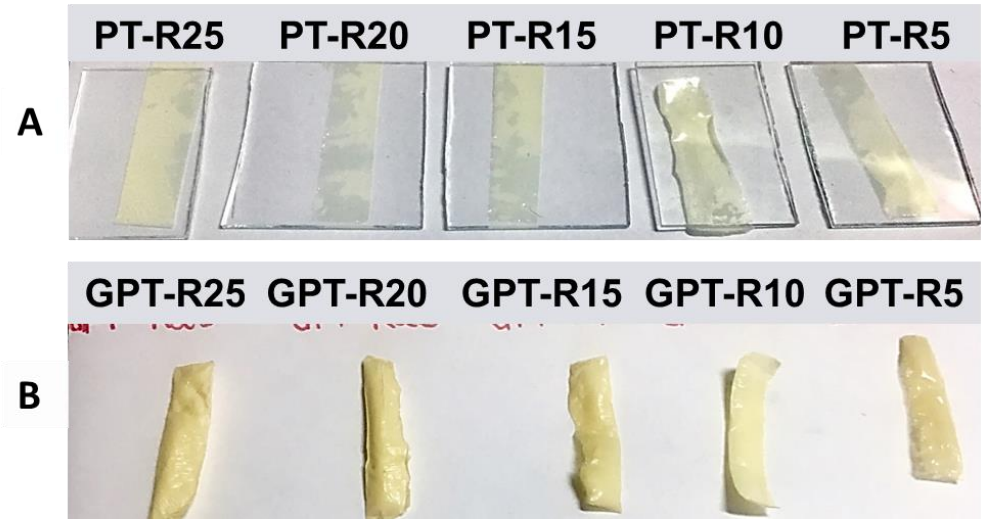

Figure 6. PVA/TiO_2 rutile membranes at TiO_2 contents (from left to right): 25%, 20%, 15%, 10% and 5%: A - membranes without crosslinked ; B – membranes crosslinked by GA.

3.2.2 SEM results

Comparing the SEM results of PVA membranes crosslinked with GA **(Figure 7)** without SBF solution immersion and SBF solution immersion for 3 weeks, we can see that there was no formation of HA on the membrane. This proves that the PVA membrane was not able to form HA in SBF.

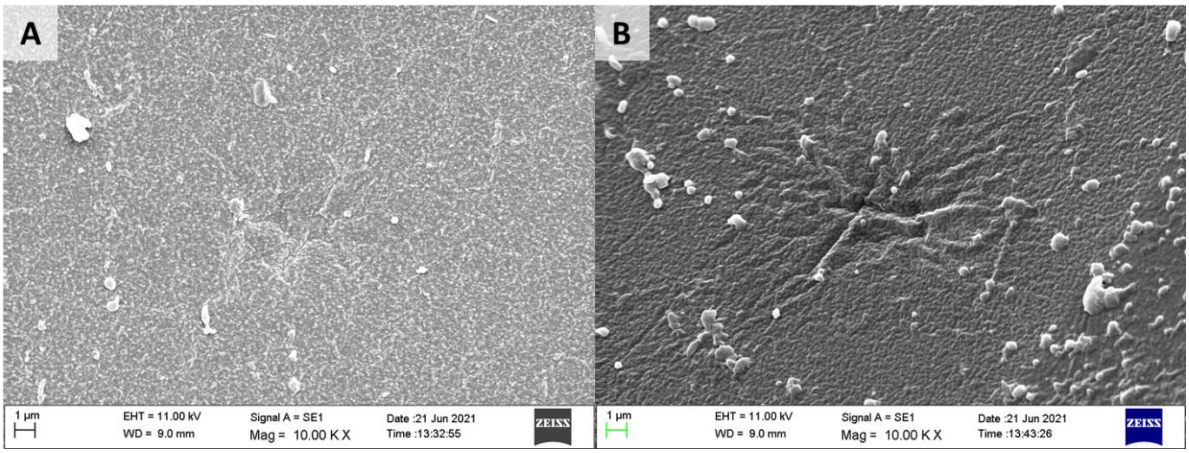

Figure 7. SEM image of GP membrane at 10000X magnification: A - no SBF immersion; B - immersed in SBF for 3 weeks.

3.3 PVA/TiO_2 anatase membrane results

3.3.1 FTIR results

IR spectra in **Figures 8**, both membranes have a wide band of about 3315 cm^{-1} related to O-H stretching, two peaks at 2940 and 2898 cm^{-1} correspond to asymmetric and symmetric vibrations of methylene groups, and another band at 1090 cm^{-1} similar to C-O stretching vibration.

According to the GA crosslinking mechanism, the OH^- groups will decrease. However, we observed that the hydroxyl group concentration does not decrease but also increases more than before crosslinking. The reason is that anatase has photocatalytic activity; UV irradiation on TiO_2 anatase surface will create a hydrophilic surface. The hydrophilicity results from the dissociation of photosynthetic water absorbing Ti^{3+} defects [5].

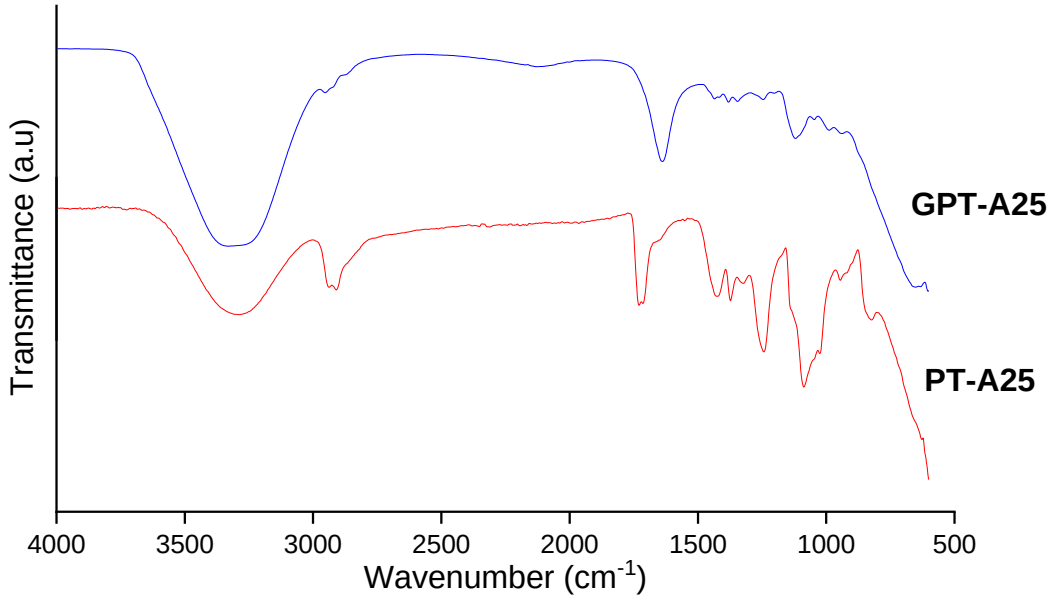

Figure 8 IR spectrum of PT-A25 membrane (red) and GPT-A25 membrane (blue)

3.3.2 SEM results

As shown in **Figure 9**, SEM of GA/PVA/TiO_2 membranes with anatase phase showed that the appearance of TiO_2 was still detected on the PVA background, but there was no HA found on the surface. We also observed that there are small-sized TiO_2 anatase particles agglomerating together makes the dispersion of particles in PVA/TiO_2 uneven and might be contributing to the subsequent formation of HA. Another reason for no appearance of HA can be lack of Ti-OH group on the surface of TiO_2. As a result, the GPT-A25 membrane was opted out from the biocompatibility test of HA/PVA/TiO_2 membranes with human skin fibroblasts.

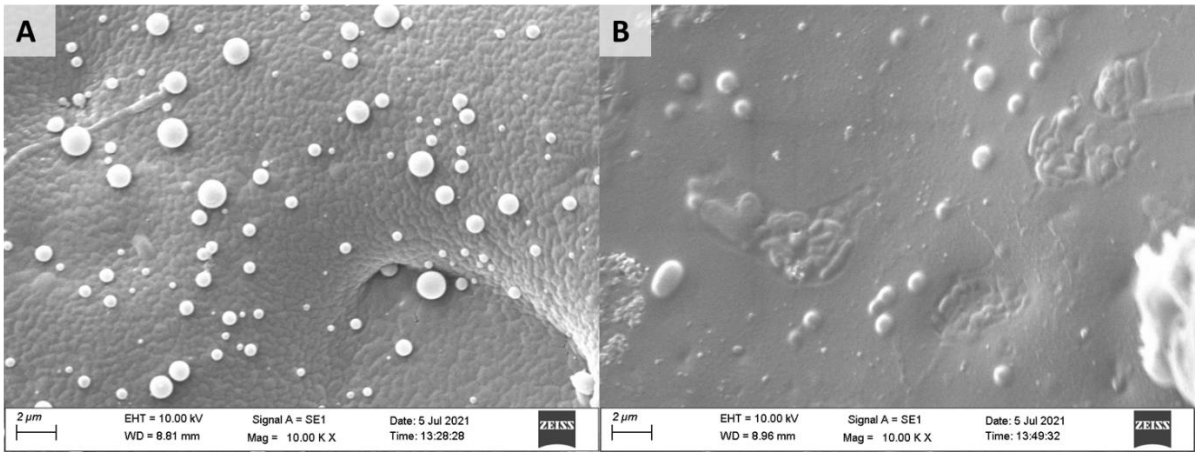

Figure 9 SEM images of GPT-A25 membrane at 10000X magnification: A - without SBF; B- immersed SBF for 3 weeks.

From the above results and comments, we found no HA formation on the GP and GPT-A membranes. Therefore, from the above issue and to ensure the experimental time is as expected, we decided to focus on research and interpretation of the results based on the rutile-phase TiO_2, especially at the TiO_2 content of 25%. The binding mechanisms and results will also be explained in the following sections.

3.4 PVA/TiO_2 rutile membrane results

3.4.1 FTIR results

The results of IR spectroscopy in **Figure 10** show a wide band of about 3315 cm^{-1} associated with O-H stretching, two peaks at 2940 and 2898 cm^{-1} corresponding to asymmetric and symmetric stretching of the methylene groups, and another peak at 1090 cm^{-1} due to C-O stretching. **Figure 10**, the hydroxyl group at 3315 cm^{-1} is reduced in intensity, at 1718 cm^{-1} appears the aldehyde group and 1097 cm^{-1} is specific for the acetal group, in the range 2940 cm^{-1} corresponds to the methylene group.

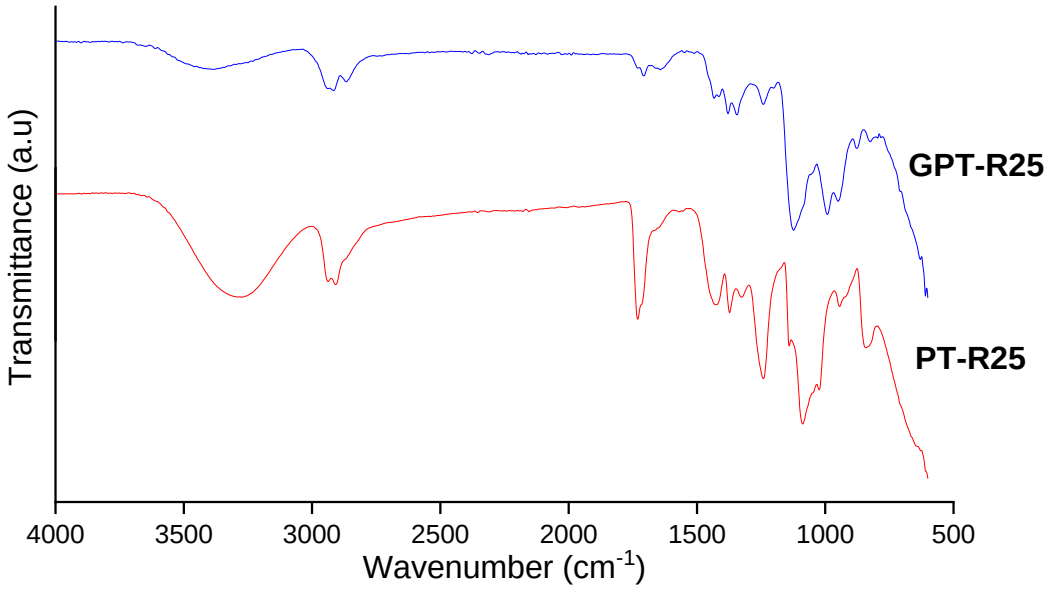

Figure 10 IR spectrum of PT-R25 membrane (red) and GPT-R25 membrane (blue)

We observed a relative decrease in the amount of hydroxyl groups upon the addition of GA to the spreading solution, which suggests that OH^- group was consumed in the reaction. However, the increase in the peak of the aldehyde was unexpected. It is less likely that GA remains in the membrane as it has been removed from the membrane through washing and drying under a vacuum. Therefore, this set of aldehyde peaks could only be evidence for nonreactive aldehydes bound to the PVA chain; that is, of the two aldehyde groups in the GA molecule, only one reacts with one chain of PVA while the other chain is not reactive, and this depends on the chain of PVA [18].

3.4.2 XRD results

X-ray diffraction is used to investigate the nanostructure and crystallization of PVA/TiO_2 membrane materials. According to previous experiments, the characteristic peak of PVA appeared at $2\theta = 19.2°$ [17]. However, **Figure 11** shows that the presence of the polymer causes

the baseline to rise higher. The characteristic peak of PVA ranges from 15° to 23°. The characteristic peaks of rutile-phase TiO_2 are aforementioned at $2\theta = 27.4^o$, 36.1^o, and 54.3^o.

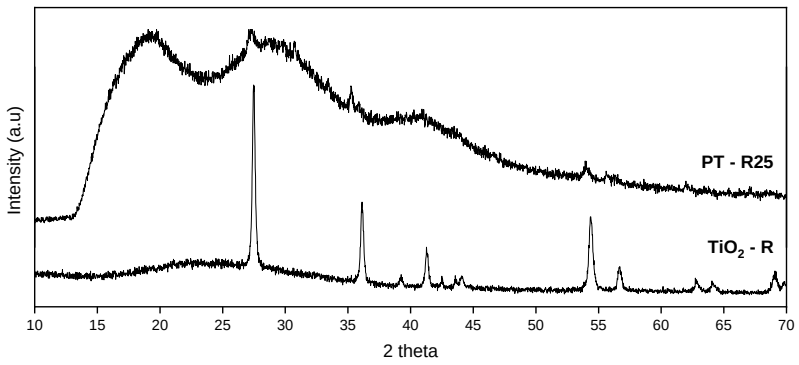

Figure 11 XRD patterns of rutile-phase TiO_2 and PT-R25 membranes (w%: 25%)

Compared with XRD diffraction of PVA [19], it is noticeable that TiO_2 doped into the PVA membrane caused the characteristic peak of PVA to increase in width and decrease in intensity. The number of hydrogen bonds formed between the PVA layers is responsible for this. The characteristic peaks do not disappear and, at the same time, appear a new peak at $2\theta = 32^o$, which is not present in both pure PVA and pure TiO_2. This means that the nanoparticles were dissociated during sonication, resulting in the interaction between PVA and TiO_2 through bonds hydrogen bonding. At the same time, this interaction also explains the decrease in intermolecular interactions of the PVA chains leading to a decrease in the degree of crystallization of PVA. The interaction between PVA and TiO_2 is because Ti^+ ions interact with the hydroxyl groups present in the PVA chain [7].

3.4.3 SEM results

Figure 12 shows the SEM image of the PT-R25 membrane after synthesis. First, the appearance of spherical TiO_2 particles on the PVA matrix supports the thesis that TiO_2 interacts with PVA through hydrogen bonding. Next, the SEM results in **Figure 13** show that the GPT-R25 membrane has the PVA matrix crosslinked, and no swelling appears, as shown in **Figure 12**. At the same time, the crosslinking process creates pores sin the membrane, which will create favourable conditions for cell growth later. In addition, spherical TiO_2 particles were observed with agglomeration sizes ranging from 20 to 50 nm.

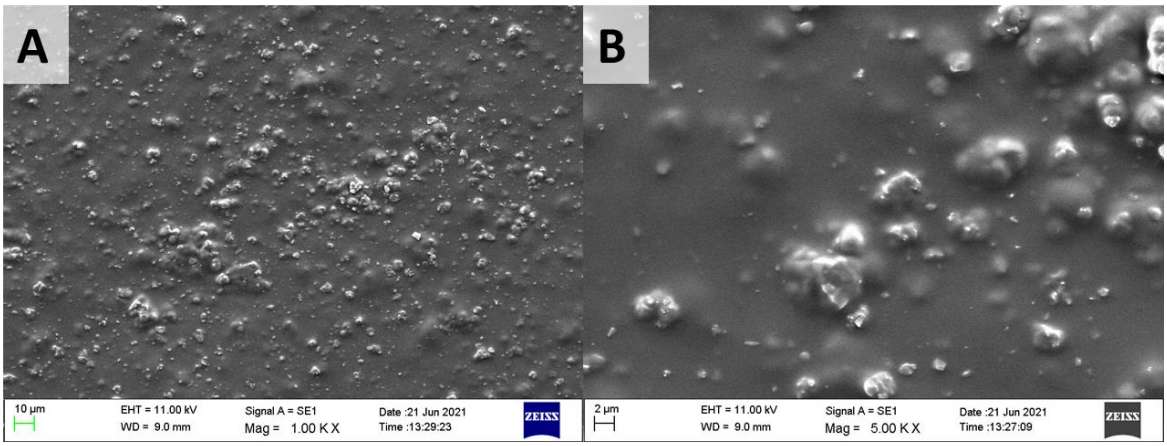

Figure 12 SEM image of PT-R25 with magnification: A – 1000X; B - 5000X.

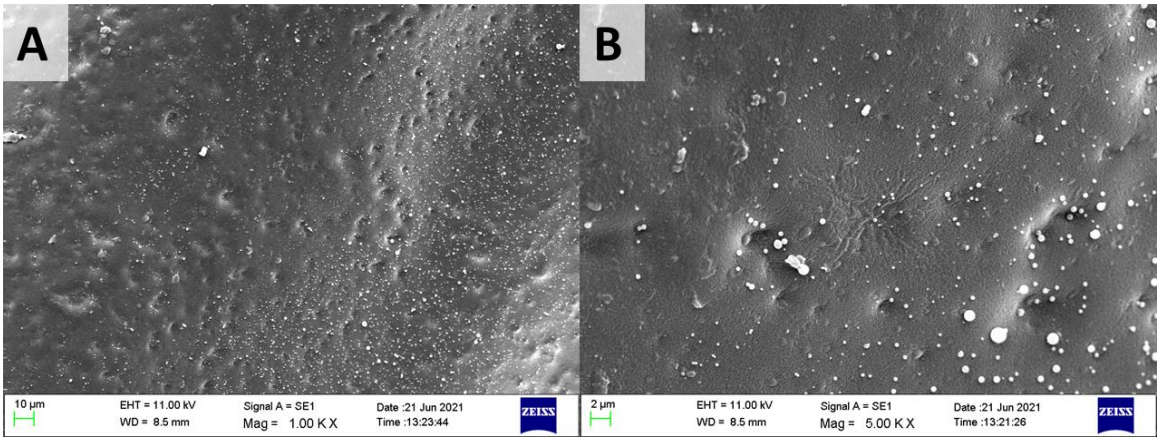

Figure 13 SEM image of GPT-R25 with magnification: A – 1000X; B - 5000X.

3.4.4 Water contact angle (WCA)

The water contact angle (WCA) is a standard method for measuring the wettability of material. The contact angle value is measured between the surface of solid material and the direct contact with the solid surface and the atmosphere. Through WCA measurement, we can predict compatibility with living cells. The lower the WCA is, the higher the membrane's wettability is. Hence, it can be a suitable environment for cell growth. WCA was performed for the PVA/TiO_2 samples in which the rutile TiO_2 had the content of 0%, 5%, 10%, 15%, 20% and 25% and the results are shown in **Figure 14**. The increase in TiO_2 percentage affects the hydrophilicity of PVA/TiO_2. The reduction of WCA means the wettability of the membranes (TiO_2 with w%: 0 - 20%) increases. However, it can be noticed that WCA of 20% PVA/TiO_2 and 25% PVA/TiO_2 have no significant difference. This might be because the maximum TiO_2 content has been gradually reached.

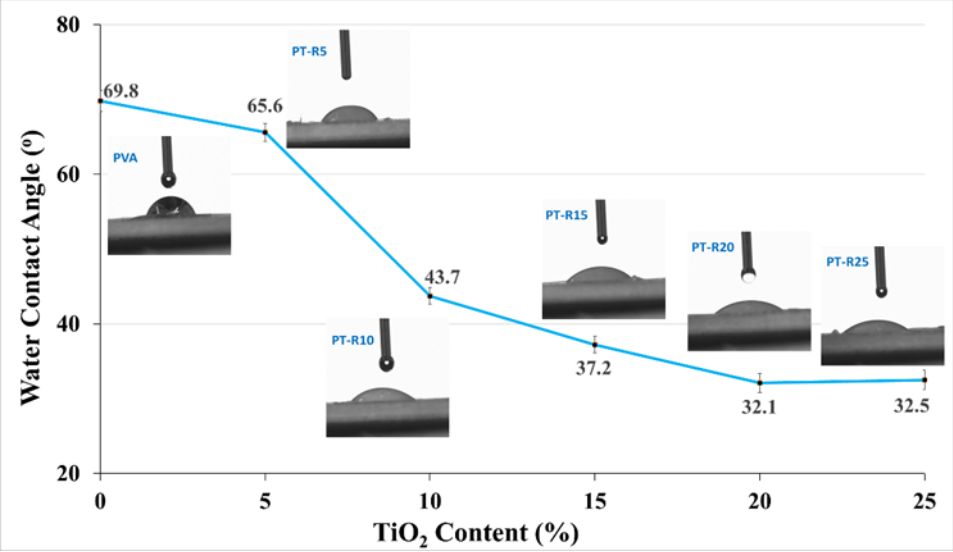

Figure 14. Water contact angle of PVA and PT-R (w%: 5 – 25%) membranes

3.4.5 The results of hydroxyapatite formation on rutile-phase PVA/TiO_2 membranes crosslinked by GA.

The formation of HA, which is dependent on surface roughness and phase composition, is also affected by the immersion time in the SBF solution. Therefore, HA formation is also an important factor in evaluating membrane biocompatibility.

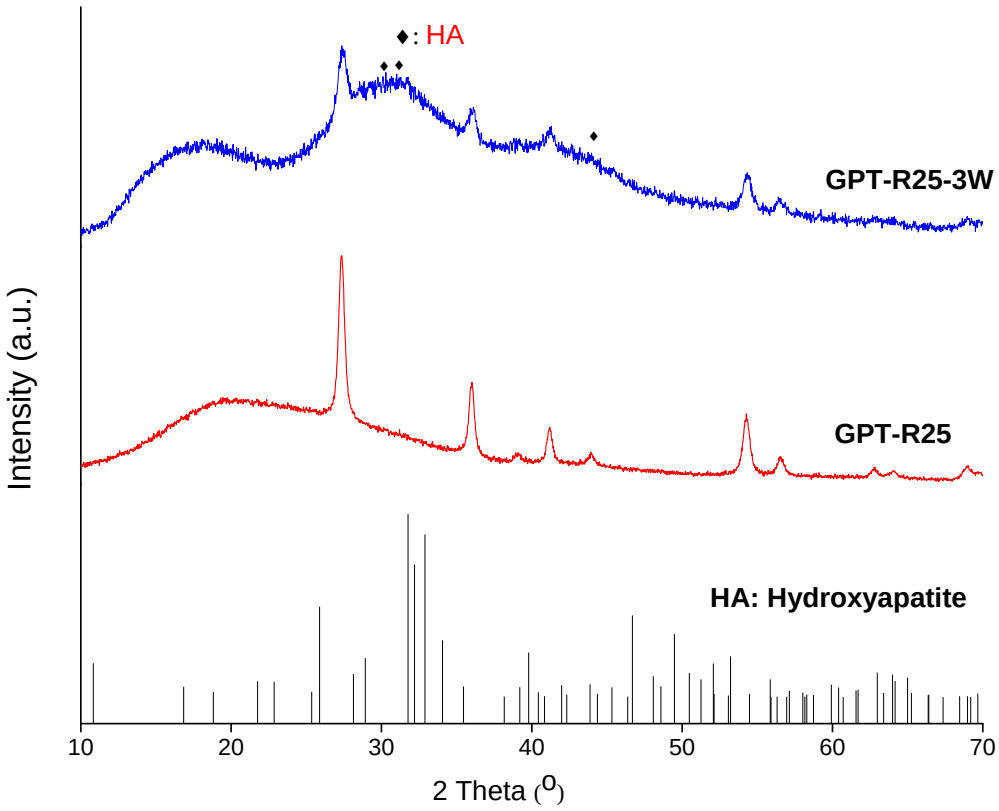

Figure 15 XRD patterns of GPT-R25 and GPT-R25-3W membranes (w%: 25%)

Figure 15 illustrates XRD powder of GPT-R25 and GPT-R25-3W membranes to demonstrate HA formation during SBF immersion. The results revealed a broad diffraction peak at 2-theta range from 31^{o} to 33^{o} which indicated characteristic signals of HA crystal at 31.7^{o}, 32.2^{o}, and 32.9^{o} corresponding to the (121), (112), and (030) planes, respectively (JCPDS No.96-901-1095). Moreover, the observation of GPT-R25-3W also predicted HA formation significantly affected on baseline intensity in XRD results.

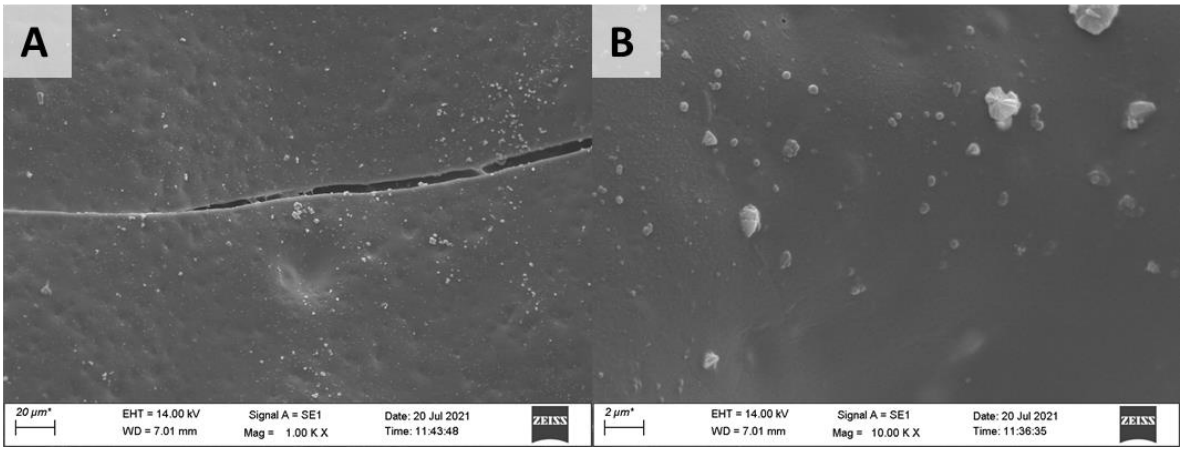

Figure 16 SEM image of GPT-R25 immersed in SBF for 1 week with magnification: A – 1000X; B - 10000X.

SEM results **(Figure 16, 17, 18)** demonstrate that HA formation gives the clearest signal in the third week, but no signal of HA is clearly visible in the first and second week. **Figure 18C** shows that the HA layer has a closely spaced structure and is stacked one after another. The specific molecular structure of HA can explain this. The Ca^{2+} of the HA molecule is located in 2 positions: (1) 4 Ca^{2+} atoms act as a bridge and connect with oxygens of phosphate groups; (2) The remaining 6 Ca^{2+} atoms bond with the remaining atoms of the phosphate groups to form equilateral triangles [1]. These links form the stacked cube-based lattice structure of HA. The pores on the membrane were also not lost when immersed in SBF, which is a positive signal for cell formation at a later stage. In addition, spherical TiO_2 particles with sizes from 20 to 30 nm were still observed at all 3 weeks.

Svetina. et al. proposed that rutile-phase TiO_2 possesses superior biocompatibility by using the first-principles molecular dynamics [20]. HA can be generated through two nucleation mechanisms when immersing TiO_2 in simulated fluid. The first way is that Ca^{2+} nucleation first on the TiO_2 surface and then the formation of inorganic calcium phosphate through the chemical bonding of Ca^{2+} with PO_4^{3-}. Another way is that Ca^{2+} ions are deposited on the TiO_2 surface terminated with OH-, as OH- can effectively induce the generation of an apatite layer on the TiO_2 surface. When the water molecules contact with the rutile (110) TiO_2 plane, they will completely dissociate because this rutile plane has a very low free energy. It leads to increase the hydrophilicity of the TiO_2 (110) plane. The OH^- ions combine with a five-coordinated titanium atom to form a terminal hydroxyl. Furthermore, H^+ will react with the bridging oxygen to form the bridging hydroxyl. Following the thermodynamic theory, the result shows that Ca^{2+} will react instead of H^+ on the TiO_2 (110) plane, followed by the attraction of PO_4^{3-} to form apatite, enhancing the biocompatibility of the TiO_2 (110) plane.

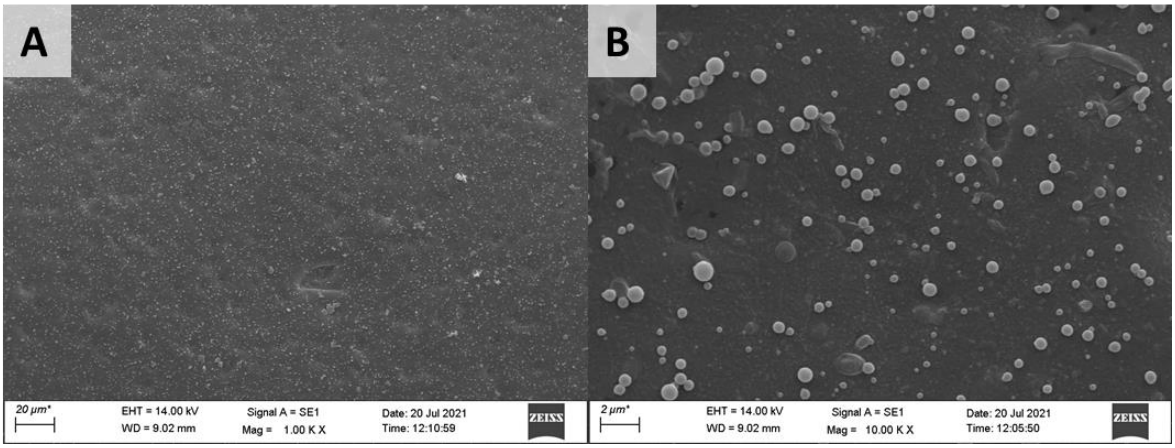

Figure 17 SEM image of GPT-R25 immersed in SBF for 2 weeks with magnification: A – 1000X; B - 10000X.

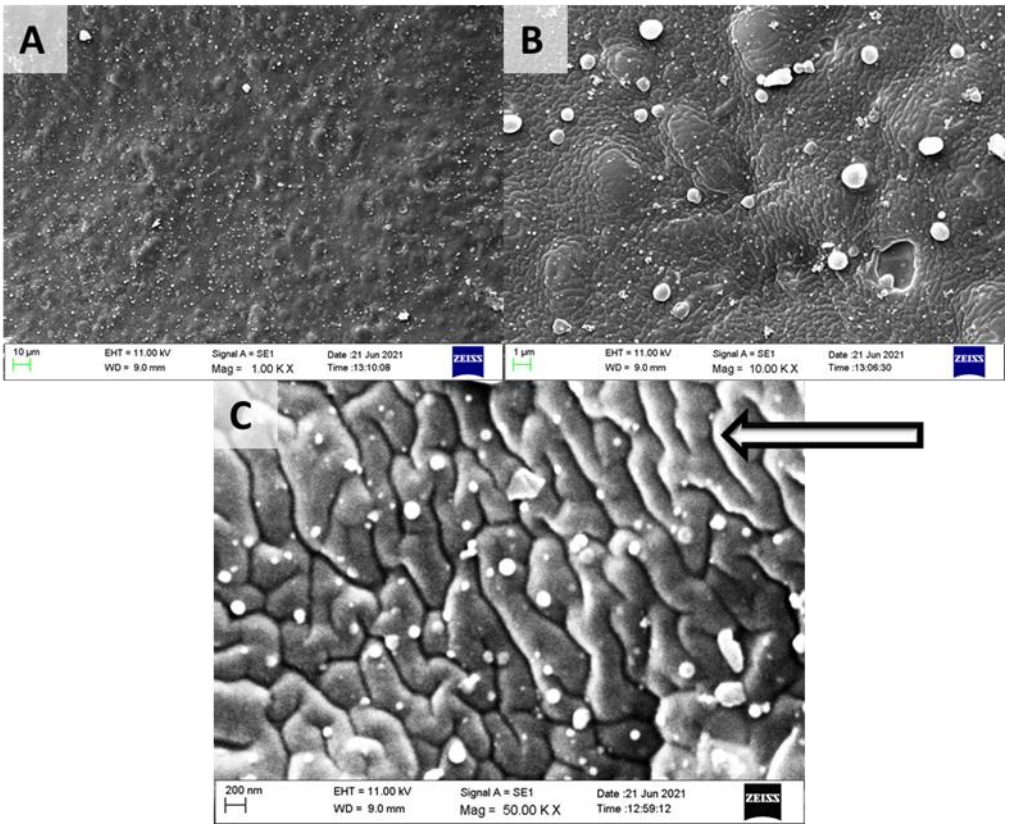

Figure 18 SEM images of GPT-R25 immersed in SBF for 3 weeks with magnification: A – 1000X; B – 10000X; C - 50000X (Structure of HA)

3.5 Cell culture results

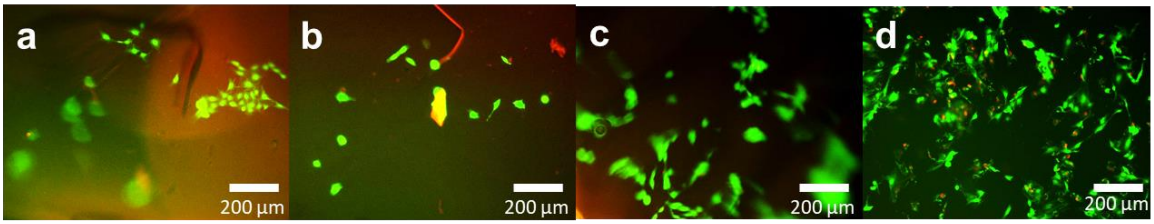

Figure 19 Fluorescence microscope images of human fibroblast cell growth after 7 days on the surface of PVA membranes crosslinked with GA: (a) without immersion in SBF; (b - d) immerse in SBF in 1 week, 2 weeks and 3 weeks, respectively. Scale bar: 200 µm

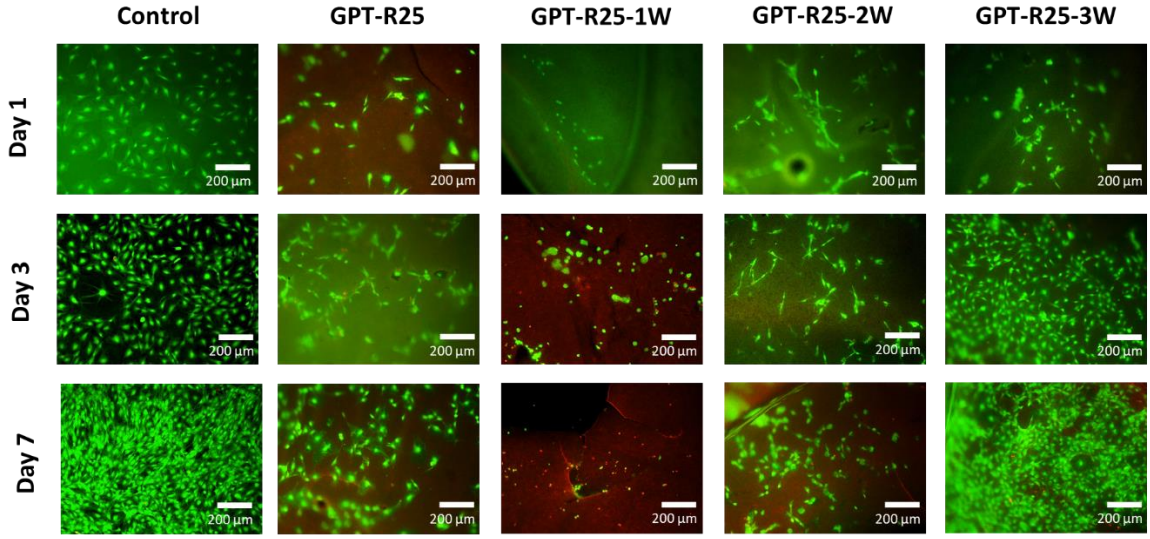

Figure 20 Fluorescence microscope images of human fibroblast cell growth after 1 day, 3 days and 7 days in control sample and on the surface of PVA/TiO_2 rutile membranes (w%: 25%) crosslinked with GA: without immersion in SBF (GPT-R25) and immerse in SBF: GPT-R25-1W, GPT-R25-2W and GPT-R25-3W in 1 week, 2 weeks and 3 weeks, respectively. Scale bar: 200 µm

GA/PVA and GA/PVA/TiO_2 rutile membranes are the samples for human skin fibroblasts *in vitro* cell culture. Therefore, cell culture on the GA/PVA and GA/PVA/TiO_2 rutile membranes was performed to determine whether these membranes support the proliferation of living cells, which is the premise for carrying out the experiments in the following studies.

Different membranes have the potential to influence the viability of human skin fibroblasts. The differences between membranes induce different HA formations, further affecting cell growth and proliferation. **Figure 19** showed that the number of cells in the GP membranes grew proportionally up to the time these membranes were immersed in SBF. It could be explained that the residual amount of GA released affects the viability of fibroblasts. The longer time the membranes were immersed in SBF, the more amount the GA residue was released. Therefore, the membrane with the lower residual amount of GA can demonstrate better cell growth due to the cytotoxic effects of GA upon cells in tissue culture [21].

Comparing the results of GA/PVA membranes with GPT-R25 membranes from **Figure 19** and **Figure 20**, it was found that there was a similarity in the growing trend of cells in SBF-immersed samples. However, on the membrane immersed in SBF for 1 week, after 3 days of cell culture, the number of dead cells increased significantly, and the live cells were much less than in the control group and GPT-R25 membrane samples without SBF. Compared with the

non-immersed and immersed samples in SBF at other immersion duration (Figures 13A, 15A, 16A and 17A), the pores on the membrane immersed for one week, causing its surfaces no longer rough enough to support cell attachment. In tissue engineering, the rough matrix acts as a temporary scaffold for tissue regeneration through cell adhesion, proliferation, and differentiation. From the second week of membrane SBF immersion, the interaction between the membrane and the solution made TiO_2 begin to appear more on the membrane surface. Rutile-phase TiO_2 with high surface energy can enhance cell adhesion and attract more cells to the surface. Therefore, with GPT-R25-2W and GPT-R25-3W membranes, the proliferation of cells after 7 days of cell culture was observed and cultured, notably with GPT-R25-3W membranes. As analyzed in the previous section, in all the rutile phases, GA/PVA and GA/PVA/TiO_2 membrane samples (w%: 25%) soaked in SBF solution at different time points, only GA/PVA/TiO_2 in the rutile phase (w%: 25%) had HA formation. Therefore, it can be shown that the presence of TiO_2 and the immersion of GPT membranes in SBF for 3 weeks are favourable conditions for human skin fibroblasts to grow.

Furthermore, the stability of cross-linked PVA in the biological environment will depend on the PVA-GA ratio and experimental conditions. Considering the application of cross-linked PVA in delivery drugs, the changing experimental conditions of the PVA cross-linked reaction produce a material, which can cover the drug. In this test, the material was immersed in a 6.8 buffer solution and PVA-GA ratios leading to decomposition were also studied in this test. On the other hand, in our test, cross-linked PVA/TiO_2 was immersed in SBF solution with a solvent of deionized water, the results showed that cross-linked PVA did not disintegrate (Figure 4). However, the limitation of this study is that the immersion test period is only up to 3 weeks. Given this period, we cannot conclude that the material will not disintegrate at all if time is increased.

They carried out the test of degradation in a pH 4.5 buffer that replicates the lysosomal environment and found that the rutile form released titanium ions less than the anatase form (120-fold lower than anatase) [22]. Because titanium ions are poorly eliminated and can accumulate over the lifetime causing effects on multiple organs [23], this significant finding may help to explain the major toxicity of TiO_2, which seemed to depend on pH, but was not seen at neutral pH [22]. Therefore, at the pH of simulated body fluid - pH = 7.4 as we tested, TiO_2 may not release titanium ions which are toxic to the body. In addition, TiO_2 nanoparticles have extremely low absorption in the body, and the high percentage of titanium dioxide is detected in the feces [24, 25].

4 Conclusion

Rutile and anatase TiO_2 powders were prepared by the sol-gel method based on the control of the acidic medium (CH_3COOH) and basic (NH_4OH) medium, respectively. At the membrane-forming stage, the hydrophilicity of PVA decreased when crosslinked with glutaraldehyde. Membranes containing rutile TiO_2 had better properties than membranes containing anatase TiO_2. The pores created on the membrane containing rutile TiO_2 supported cell adhesion and growth, especially on membranes with 25% TiO_2. In addition, according to WCA values, the maximum TiO_2 content has been gradually reached from this content. There was also a clear difference between the PVA/TiO_2 rutile and anatase membranes in the formation of HA. In the rutile membranes, the presence of HA was clearly observed at the third week, while there was no such appearance in the anatase ones. The mechanism of HA formation has also been explained based on the rutile (110) plane characteristics. HA formation on PVA/TiO_2 rutile membrane (w%: 25%) undoubtedly plays an essential role in the viability of human dermal fibroblasts.

Acknowledgement

This research is funded by University of Science, Vietnam National University – Ho Chi Minh City (VNU-HCM) under grant number T2022-15. The authors would like to thank Ms. Fiona Verisqa for the proof-reading.

References

1. Orlovskii V, Komlev V, Barinov S. Hydroxyapatite and hydroxyapatite-based ceramics. Inorganic materials. 2002;38(10):973-84.
2. Szcześ A, Hołysz L, Chibowski E. Synthesis of hydroxyapatite for biomedical applications. Advances in colloid and interface science. 2017;249:321-30.
3. Nayak AK. Hydroxyapatite synthesis methodologies: an overview. International Journal of ChemTech Research. 2010;2(2):903-7.
4. Jaafar A, Hecker C, Árki P, Joseph Y. Sol-gel derived hydroxyapatite coatings for titanium implants: A review. Bioengineering. 2020;7(4):127.
5. Kasuga T, Kondo H, Nogami M. Apatite formation on TiO2 in simulated body fluid. Journal of Crystal Growth. 2002;235(1-4):235-40.
6. Benčina M, Iglič A, Mozetič M, Junkar I. Crystallized TiO2 nanosurfaces in biomedical applications. Nanomaterials. 2020;10(6):1121.
7. Shehap A, Akil DS. Structural and optical properties of TiO 2 nanoparticles/PVA for different composites thin films. International Journal of Nanoelectronics & Materials. 2016;9(1).
8. Sadat-Shojai M, Khorasani M-T, Dinpanah-Khoshdargi E, Jamshidi A. Synthesis methods for nanosized hydroxyapatite with diverse structures. Acta biomaterialia. 2013;9(8):7591-621.
9. Tsuchiya H, Macak JM, Müller L, Kunze J, Müller F, Greil P, et al. Hydroxyapatite growth on anodic TiO2 nanotubes. Journal of Biomedical Materials Research Part A: An Official Journal of The Society for Biomaterials, The Japanese Society for Biomaterials, and The Australian Society for Biomaterials and the Korean Society for Biomaterials. 2006;77(3):534-41.
10. Niranjan R, Kaushik M, Selvi RT, Prakash J, Venkataprasanna K, Prema D, et al. PVA/SA/TiO2-CUR patch for enhanced wound healing application: In vitro and in vivo analysis. International journal of biological macromolecules. 2019;138:704-17.
11. Kokubo T, Takadama H. How useful is SBF in predicting in vivo bone bioactivity? Biomaterials. 2006;27(15):2907-15.
12. Hsiao I-L, Huang Y-J. Effects of various physicochemical characteristics on the toxicities of ZnO and TiO2 nanoparticles toward human lung epithelial cells. Science of the total environment. 2011;409(7):1219-28.
13. Zhang Q, Gao L, Guo J. Effect of hydrolysis conditions on morphology and crystallization of nanosized TiO2 powder. Journal of the European Ceramic Society. 2000;20(12):2153-8.
14. Zhu Y, Zhang L, Gao C, Cao L. The synthesis of nanosized TiO2 powder using a sol-gel method with TiCl4 as a precursor. Journal of Materials Science. 2000;35(16):4049-54.
15. Figueiredo KC, Alves TL, Borges CP. Poly (vinyl alcohol) films crosslinked by glutaraldehyde under mild conditions. Journal of applied polymer science. 2009;111(6):3074-80.
16. Kang M-S, Kim JH, Won J, Moon S-H, Kang YS. Highly charged proton exchange membranes prepared by using water soluble polymer blends for fuel cells. Journal of Membrane Science. 2005;247(1-2):127-35.

17. Qin X, Dou G, Jiang G, Zhang S. Characterization of poly (vinyl alcohol) nanofiber mats cross-linked with glutaraldehyde. Journal of Industrial Textiles. 2013;43(1):34-44.
18. Yeom C-K, Lee K-H. Pervaporation separation of water-acetic acid mixtures through poly (vinyl alcohol) membranes crosslinked with glutaraldehyde. Journal of membrane science. 1996;109(2):257-65.
19. Aziz SB, Abdulwahid RT, Rasheed MA, Abdullah OG, Ahmed HM. Polymer blending as a novel approach for tuning the SPR peaks of silver nanoparticles. Polymers. 2017;9(10):486.
20. Tsou HK, Hsieh PY, Chi MH, Chung CJ, He JL. Improved osteoblast compatibility of medical-grade polyetheretherketone using arc ionplated rutile/anatase titanium dioxide films for spinal implants. Journal of Biomedical Materials Research Part A. 2012;100(10):2787-92.
21. Speer DP, Chvapil M, Eskelson C, Ulreich J. Biological effects of residual glutaraldehyde in glutaraldehyde-tanned collagen biomaterials. Journal of biomedical materials research. 1980;14(6):753-64.
22. De Matteis V, Cascione M, Brunetti V, Toma CC, Rinaldi R. Toxicity assessment of anatase and rutile titanium dioxide nanoparticles: The role of degradation in different pH conditions and light exposure. Toxicology in vitro. 2016;37:201-10.
23. Luo Z, Li Z, Xie Z, Sokolova IM, Song L, Peijnenburg WJ, et al. Rethinking nano-TiO2 safety: overview of toxic effects in humans and aquatic animals. Small. 2020;16(36):2002019.
24. Cho W-S, Kang B-C, Lee JK, Jeong J, Che J-H, Seok SH. Comparative absorption, distribution, and excretion of titanium dioxide and zinc oxide nanoparticles after repeated oral administration. Particle and fibre toxicology. 2013;10(1):1-9.
25. MacNicoll A, Kelly M, Aksoy H, Kramer E, Bouwmeester H, Chaudhry Q. A study of the uptake and biodistribution of nano-titanium dioxide using in vitro and in vivo models of oral intake. Journal of Nanoparticle Research. 2015;17(2):1-20.